Relaxation and edge reconstruction in integer quantum Hall systems

2012 New J. Phys. 14 105009

(http://iopscience.iop.org/1367-2630/14/10/105009)

New Journal of Physics
The open-access journal for physics

Relaxation and edge reconstruction in integer quantum Hall systems

Torsten Karzig[1,4], Alex Levchenko[2], Leonid I Glazman[3] and Felix von Oppen[1]

[1] Dahlem Center for Complex Quantum Systems and Fachbereich Physik, Freie Universität Berlin, 14195 Berlin, Germany
[2] Department of Physics and Astronomy, Michigan State University, East Lansing, MI 48824, USA
[3] Department of Physics, Yale University, 217 Prospect Street, New Haven, CT 06520, USA
E-mail: Torsten.Karzig@fu-berlin.de

New Journal of Physics **14** (2012) 105009 (14pp)
Received 1 June 2012
Published 10 October 2012
Online at http://www.njp.org/
doi:10.1088/1367-2630/14/10/105009

Abstract. The interplay between the confinement potential and the electron–electron interactions causes reconstructions of quantum Hall edges. We study the consequences of this edge reconstruction for the relaxation of hot electrons injected into integer quantum Hall edge states. In translationally invariant edges, the relaxation of hot electrons is governed by three-body collisions, which are sensitive to the electron dispersion and thus to reconstruction effects. We show that the relaxation rates are significantly altered in different reconstruction scenarios.

[4] Author to whom any correspondence should be addressed.

Contents

1. Introduction

The kinetic properties of one-dimensional (1D) quantum systems are an active area of current research [1, 2]. What makes the field exciting is that many-particle physics is drastically different in one spatial dimension. This difference is already evidenced in basic nonequilibrium properties such as the microscopic mechanisms of relaxation. Within the scope of Fermi-liquid theory, relaxation processes in higher dimensions proceed by pair collisions of electrons, which provide an efficient mechanism for the relaxation of initial nonequilibrium states. In contrast, conservation of energy and momentum strongly restricts scattering in one spatial dimension so that pair collisions necessarily result in zero-momentum exchange or an interchange of the momenta of the colliding particles. Neither process causes relaxation. This poses the fundamental question of the microscopic origin of relaxation in 1D systems. Notably, the absence of relaxation by pair collisions, which holds true regardless of the strength of interaction, has received experimental support [3].

The question of equilibration emerges in a diverse set of 1D many-body systems. These include energy and momentum-resolved tunneling experiments with nanoscale quantum wires [3, 4], quench dynamics of cold atomic gases [5, 6] as well as energy-spectroscopy experiments on quantum Hall edge states driven out of equilibrium [7–10]. This paper is motivated by the latter experiments, which were carried out in a high-mobility two-dimensional electron system at Landau-level filling factor $\nu = 2$. This system hosts two co-propagating edge states, which can be driven out of equilibrium by inter-edge tunneling in the vicinity of quantum point contacts. This generates a nonequilibrium distribution of electron energy (in the sense of electronic edge transport) downstream from the contact, which is monitored as a function of the propagation distance by means of a quantum-dot-based energy spectrometer. The experiments show that the initial nonequilibrium distribution relaxes to a stationary form that is close to the thermal distribution but with an effective temperature and chemical potential.

Edge-state equilibration was also probed in experiments at Landau-level filling factor $\nu = 1$ [11]. Heat is carried unidirectionally by the single chiral edge mode as confirmed by thermopower measurements along the edge. These experiments found that hot electrons injected locally into the edge cool down while propagating along the edge. It is worth emphasizing that

the standard chiral-Luttinger-liquid model for quantum Hall edge states [12] does not account for equilibration effects. Indeed, this model is exactly solvable and, as usual, its integrability is an obstacle to thermalization. In early works [13] this apparent difficulty was overcome by assuming a disordered edge where impurity-mediated scattering allows for interchannel equilibration.

These experimental discoveries led to a flurry of theoretical activity. We briefly summarize these contributions and place our work in their context. Two early publications [14, 15] used entirely different concepts. The work by Lunde *et al* [14] was based on a Boltzmann kinetic equation for a disordered edge. Since translation invariance is broken, momentum is no longer a good quantum number and relaxation becomes possible even by two-particle collisions. Degiovanni *et al* [15] adopted a bosonization approach and combined it with a phenomenological model for the plasmon distribution generated at the quantum point contact. Within this model, thermalization was interpreted to be a consequence of plasmon dispersion, which causes the electron wave packets to broaden as they propagate with different group velocities. This picture was elegantly elaborated and extended in [16–18]. A third mechanism was proposed in the context of electronic Mach–Zehnder interferometers [19, 20] based on electron–plasmon scattering [21]. This mechanism relies on the scattering of high-energy electrons by low-energy plasmons enabled by the curvature of the fermionic spectrum.

Despite the insight provided by these theories, important issues need to be sorted out. First, these works do not give a definitive answer to the question whether relaxation is possible in translationally invariant clean edges. Specifically, the dispersion of plasmon modes may lead to a steady state but does not constitute true relaxation as the energy in each plasmon mode is conserved. Second, the edge of quantum Hall systems can be reconstructed due to Coulomb interactions. The precise nature of reconstruction depends on the steepness of the confinement potential, ranging from no reconstruction for very sharp confinement potentials [22] to alternating compressible and incompressible stripes for very smooth edges [23]. Indeed, experiments [24, 25] point to an important role of reconstruction effects in energy transfer along the edge.

The purpose of this paper is to address these issues within minimal models of unreconstructed and reconstructed edges. Specifically, we consider energy relaxation of a hot particle injected into translationally invariant quantum Hall edges at Landau-level filling factors $\nu = 1, 2$. With the assumption that the velocity v_1 of the injected particle differs sufficiently from the Fermi velocity v_F, we treat the Coulomb interaction perturbatively [26, 27]. In this limit, relaxation processes are dominated by three-body collisions which depend sensitively on the electron dispersion and hence on the edge reconstruction. We begin with a discussion of energy relaxation for the unreconstructed edge in section 2. We then discuss two simple models of reconstructed quantum Hall edges. In section 3, we discuss relaxation processes for a spin-reconstructed edge for filling factor $\nu = 2$. In section 4, we turn to a minimal model of charge reconstruction of a $\nu = 1$ edge, which provides the simplest realization of counter-propagating edge modes. We conclude in section 5.

2. Unreconstructed edge

A confinement potential $V_c(x)$ that is sharp on the scale of the Coulomb interaction (i.e. $V_c' \gg e^2/(\kappa l_B^2)$, where κ is the dielectric constant and l_B denotes the magnetic length) remains stable against interaction-induced reconstructions and the electron dispersion $\varepsilon(k)$

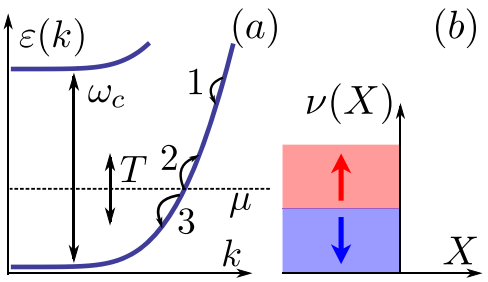

Figure 1. Edge without reconstruction effects. (a) Single-particle dispersions and typical relaxation processes in the the lowest Landau level for a spin degenerate system. Vertical arrows label temperature T and cyclotron energy $\omega_c = eB/m$. Panel (b) shows the corresponding sharp ($T = 0$) occupation number in terms of the guiding center position X.

can be obtained approximately from the noninteracting Schrödinger equation [22]. A generic electronic dispersion of an unreconstructed edge is sketched in figure 1(a), exhibiting a confinement-induced bending of the Landau levels near the edge of the sample.

In the limit of high magnetic fields ($V_c' \ll \omega_c/l_B$), the electron states near the edge can be described by the lowest Landau-level wave functions

$$\psi_X(x, y) = (Ll_B\sqrt{\pi})^{-1/2} e^{-iky} e^{-(x-X)^2/2l_B^2} \tag{1}$$

in the Landau gauge. Here, $k = X/l_B^2$ and L denotes the length of the sample edge (taken along the y direction). The defining feature of the unreconstructed edge is the sharp zero-temperature occupation function $\nu_\sigma(X) = \Theta(-X)$ of Landau-level states with the guiding center X when the Zeeman splitting ε_Z is negligible (see figure 1(b)).

The single-particle dispersion near the Fermi energy (corresponding to momentum k_F) is controlled by the confinement potential and can be approximated as

$$\varepsilon(k) = v_F(k - k_F) + (k - k_F)^2/2m_c. \tag{2}$$

The dispersion is parametrized through the edge velocity $v_F = V_c' l_B^2$ at the Fermi energy and the curvature $1/m_c = V_c'' l_B^4$. Note that these parameters become maximal for an infinitely sharp edge for which $v_F \sim \omega_c l_B$ and $1/m_c \sim 1/m$ [22]. Note, however, that a description in terms of the wave functions in equation (1) is no longer valid in this extreme limit.

The finite curvature of the dispersion implies that at least three particles are required for an energy and momentum conserving relaxation process. Relaxation of a high-energy electron (labeled by $i = 1$ in figure 1(a)) is possible by scattering two electrons (labeled $i = 2, 3$ in figure 1(a)) near the Fermi energy. Indeed, due to the curvature of the dispersion near the Fermi energy, exciting electron $i = 2$ from the Fermi energy requires more energy than scattering electron $i = 3$ deeper into the Fermi sea. Clearly, this relaxation process relies on finite temperature, and the typical energy transfers for electrons $i = 2, 3$ at the Fermi energy are of the order of T. Quantitatively, this process can relax the hot particle with excess energy $\varepsilon \approx v_F(k_1 - k_F) = v_F \Delta k$ by $q_1 = q_3(k_{2'} - k_3)/\Delta k$, where $q_i = k_{i'} - k_i$ is the momentum transferred to particle i in the collision. Note that $q_1 \ll q_3$ so that relaxation occurs in many small steps $v_F q_1 \sim T^2/\varepsilon$.

For Landau-level filling factor $\nu = 2$, these considerations apply when the Zeeman splitting is small compared to the temperature. In the opposite limit $\varepsilon_Z \gg T$, the curvature of the

dispersion implies that the Fermi momenta and hence the Fermi velocities differ for the two spin directions. In this case, relaxation is dominated by processes in which the electrons $i = 1$ and 2 have opposite spins and thus different Fermi momenta $k_{\mathrm{F}j}$ and Fermi velocities v_j with $j = 1, 2$. To include a finite Zeeman splitting at Landau-level filling factor $\nu = 2$ as well as for later convenience, it is thus beneficial to consider a modified dispersion

$$\varepsilon(k) = \begin{cases} v_j(k - k_{\mathrm{F}j}), & k \approx k_{\mathrm{F}j}, \\ v_1(k - k_1) + \varepsilon, & k \approx k_1, \end{cases} \tag{3}$$

which is linearized in the vicinity of each of the three particles, including the hot particle with velocity v_1 and momentum k_1. This captures the behavior in the regime of strong Zeeman splitting $\varepsilon_{\mathrm{Z}} \gg T$, which we will focus on in the following. Nevertheless, we can also recover the results for the quadratic dispersion and weak Zeeman splitting $\varepsilon_{\mathrm{Z}} \ll T$ by identifying $v_2 - v_3$ with the typical velocity difference $T/(v_{\mathrm{F}} m_{\mathrm{c}})$ due to the curvature of the dispersion.

Using the dispersion in equation (3), energy and momentum conservation leads to

$$q_1 = \frac{v_2 - v_3}{v_1 - v_2} q_3. \tag{4}$$

The velocity difference $v_2 - v_3 = \varepsilon_{\mathrm{Z}}/(v_2 m_{\mathrm{c}})$ is controlled by the Zeeman splitting, which we assume to be small compared to the excitation energy ε such that $(v_2 - v_3) \ll (v_1 - v_2)$.

2.1. Three-body scattering formalism

Energy relaxation by processes of the kind shown in figure 1(a) has already been discussed in the context of quantum wires in [26]. While our calculation here follows the same outline, there are characteristic differences related to the nature of the interaction matrix elements. The energy relaxation rate via three-body collisions is again given by

$$\frac{1}{\tau_{\mathrm{E}}} = \sum_{231'2'3'} \frac{-v_1 q_1}{\varepsilon} W^{123}_{1'2'3'} n_2 n_3 (1 - n_{1'})(1 - n_{2'})(1 - n_{3'}), \tag{5}$$

where n_i is the Fermi–Dirac distribution function at k_i. The factor involving q_1 weights the out-scattering rate with the relative relaxed energy, accounting for the fact that the hot particle relaxes only a fraction of its energy in a single collision. The three-body matrix element can be evaluated by using the generalized golden rule

$$W^{123}_{1'2'3'} = 2\pi |\langle 1'2'3'|V G_0 V|123\rangle_c|^2 \delta(E - E'). \tag{6}$$

Here, G_0 is the free Green's function, $V = (1/2L) \sum_{k_1 k_2 q \sigma_1 \sigma_2} V_q(k_1 - k_2) a^\dagger_{k_1+q\sigma_1} a^\dagger_{k_2-q\sigma_2} a_{k_2\sigma_2} a_{k_1\sigma_1}$ is the generic two-body interaction potential and the subscript c emphasizes that only connected processes contribute that involve all three particles.

The calculation for quantum Hall edges differs from that for quantum wires in the form of the Coulomb matrix element $V_q(k_1 - k_2)$, which now has to be evaluated using the Landau-level wave functions in equation (1). For quantum Hall systems, the Coulomb matrix element is exponentially suppressed by a factor of $\exp(-q^2 l_B^2/2)$ for large momentum transfers. This is particularly relevant because large momentum transfers yield the leading contribution to relaxation in quantum wires [26]. Moreover, $V_q(k_1 - k_2)$ depends not only on the momentum transfer but also on the initial momentum difference that controls the distance between the

guiding centers of the interacting electrons. Focusing on the remaining small momentum transfer processes ($q \ll 1/l_B$), one obtains (see appendix A for details)

$$V_q(k_1-k_2) \simeq \begin{cases} -\frac{2e^2}{\kappa}\ln|q l_B|, & k_1-k_2 \ll l_B^{-1}, \\ -\frac{2e^2}{\kappa}\ln|q(k_1-k_2+q)l_B^2|, & k_1-k_2 \gg l_B^{-1}, \end{cases} \tag{7}$$

with the understanding that at small q, the matrix elements will be eventually cut off by a large length scale $\lambda \gg l_B$ which is given by the distance to a screening gate. For $k_1-k_2 \ll 1/l_B$, the Coulomb matrix element is that of a quantum wire of width l_B. For $k_1-k_2 \gg 1/l_B$, the interaction is that of electrons in two quantum wires separated by a distance of $(k_1-k_2+q)l_B^2$, which is equal to the average of the guiding center distances of the electrons before and after the collision.

With the absence of large momentum transfer processes the three-body scattering is dominated by the direct matrix element. The importance of the (k_1-k_2) dependence of the Coulomb matrix element can be seen from the fact that the linearized dispersion of equation (3) leads to a vanishing direct matrix element for a quantum-wire-like Coulomb interaction $V_q(0)$ (see appendix B). In contrast, when reiterating the derivation [28] of the direct matrix element $T^{123}_{1'2'3'}$ including the dependence of $V_q(k_1-k_2)$ on the initial momenta, the result does *not* vanish and takes the form

$$T^{123}_{1'2'3'} = -\frac{2e^2}{L^2\kappa}\left(\frac{k_2-k_3}{v_2-v_3}\frac{V_{q_3}(k_2-k_3)}{(\Delta k)^2} - \frac{2V_{q_3}(\Delta k)}{(v_1-v_2)\,(\Delta k)} + \frac{v_2-v_3}{k_2-k_3}\frac{V_{q_1}(\Delta k)}{(v_1-v_2)^2}\right). \tag{8}$$

Here we used $k_1-k_2 \approx k_1-k_{F2} = \Delta k$. This expression is applicable under the assumption that all initial momentum differences are large compared to $1/l_B$ to also suit the reconstruction effects that will be discussed later. For the unreconstructed edge, it is however more reasonable to assume $k_2-k_3 \ll 1/l_B$ (for typical $\varepsilon_Z, T \ll e^2/\kappa l_B$), in which case the last term of equation (8), involving V_{q_1}, does not show up (see appendix B).

2.2. *Results for the unreconstructed edge*

For the unreconstructed edge, the momentum and velocity differences are linked by the curvature of the confinement potential via $v_2-v_3 = (k_2-k_3)/m_c$ and $v_1-v_2 = \Delta k/m_c$. The direct matrix element then takes the form

$$T^{123}_{1'2'3'} = -\frac{2e^2 m_c}{L^2\kappa(\Delta k)^2}\left[V_{q_3}(k_2-k_3) - 2V_{q_3}(\Delta k)\right]. \tag{9}$$

Since for large Zeeman energy the particles at k_2 and k_3 have opposite spins, there is no exchange contribution (remember that exchange is appreciable for small momentum transfers only) and equation (9) fully determines the three-body matrix element. The corresponding energy relaxation rate can then be obtained by power counting, which yields

$$\frac{1}{\tau_E} \sim m_c(v_2-v_3)^2\left(\frac{e^2}{\kappa v_2}\right)^4 \frac{(m_c v_1^2)^4\, T^4}{\varepsilon^8}. \tag{10}$$

Here $1/m_c = V_c'' l_B^4$, $(v_2-v_3) = \varepsilon_Z/(v_2 m_c)$ and we also used $\Delta k = m_c(v_1-v_2) = \varepsilon/v_1$. In obtaining equation (10), a factor of $L/(v_1-v_2)$ emerges from eliminating the energy δ-function in equation (5), each summation over the remaining k_2, k_3, q_3 contributes a phase space factor of $\sim T/v_2$ and the weighting factor $v_1 q_1/\varepsilon$ takes the form $v_1(v_2-v_3)T/[v_2(v_1-v_2)\varepsilon]$. Finally, we have to account for the competition between excitation ($q_1 > 0$) and relaxation ($q_1 < 0$) of

the hot particle. The latter is slightly favored because the momentum transfer working against the Fermi distribution is reduced by a fraction $v_2 q_1/T \sim (v_2 - v_3)/(v_1 - v_2)$.

Equation (10), valid at $\varepsilon \gg m_c v_1 e^2/\kappa$ and $\varepsilon_Z \gg T$, implies that the relaxation rate is strongly temperature dependent and can be enhanced by increasing the magnetic field.

As mentioned above, the relaxation rate in the opposite limit of weak Zeeman splitting $\varepsilon_Z \ll T$ can be obtained up to prefactors by replacing $(v_2 - v_3) \sim T/(v_2 m_c)$. Note that this regime allows for a small momentum transfer exchange term $T^{123}_{1'3'2'}$ because particles 2 and 3 are no longer necessarily of opposite spin. $T^{123}_{1'3'2'}$ can then be obtained from equation (9) by replacing $q_3 \to k_{2'} - k_3$, which does not change the power counting argument.

It is therefore possible to combine both cases by setting $v_2 - v_3 = \max\{\varepsilon_Z, T\}/(v_2 m_c)$. In the case of $v_1 \approx v_2 = V_c' l_B^2$, it is then possible to rewrite equation (10) as

$$\frac{1}{\tau_E} \sim \frac{\max\{\varepsilon_Z, T\}^2}{V_c'' l_B^2} \left(\frac{V_c'}{V_c'' l_B}\right)^2 \left(\frac{e^2}{\kappa l_B}\right)^4 \frac{T^4}{\varepsilon^8}, \tag{11}$$

which applies for the regime $V_c' l_B^2 \gg \varepsilon (V_c'' l_B^2/V_c') \gg e^2/\kappa$.

For a later comparison of the relaxation rates before and after edge reconstruction, it will be useful to consider the unreconstructed case as the $v_1 \gg v_2 \sim e^2/\kappa$ limit of equation (10) (which can be applied for $\varepsilon \gg (e^2/\kappa l_B)^2/(V_c'' l_B^2)$). Formally, this regime leaves the condition for applicability of the Taylor expansion of the confinement potential that defines $1/m_c = V_c''(\mu) l_B^4$ and would lead to another inverse mass $V_c''(\mu + \varepsilon) l_B^4$ for curvature effects at energies of the order of ε. Distinguishing these different masses does not, however, lead to qualitative changes in the results, and for brevity of the presentation we assume a quadratic confinement potential over the energy interval $[\mu, \mu + \varepsilon]$. We can then rewrite equation (10) as

$$\frac{1}{\tau_E^{(u)}} \sim \left(\frac{\max\{\varepsilon_Z, T\}}{e^2/(\kappa l_B)}\right)^2 (V_c'' l_B^2) \left(\frac{T}{\varepsilon}\right)^4, \tag{12}$$

where we used that in this regime, $m_c v_1^2 \sim \epsilon$. The crossover between equations (11) and (12) can be obtained at their limits of applicability by setting $\varepsilon = e^2 V_c'/(\kappa l_B^2 V_c'')$ and $V_c' = e^2/(\kappa l_B^2)$.

Note that for a spin polarized edge, equations (10)–(12) apply only if the Coulomb interaction is not screened for momenta of the order of T/v_2. For a screened short-range interaction ($T/v_2 \ll 1/\lambda$), the Pauli principle then leads to a suppression of the energy relaxation rate by an additional factor of $(T\lambda/v_2)^4 \ll 1$ [27].

3. Spin reconstruction

The edge reconstruction in quantum Hall systems results from competition between the Coulomb interaction and the confinement potential. Spin reconstruction at $\nu = 2$ takes place when the confinement potential V_c varies sufficiently slowly so that $V_c' < e^2/\kappa l_B^2$ and can be understood at the level of the Hartree–Fock approximation [29–32]. Once the slope of the confinement potential becomes weaker than that of the repulsive Hartree potential V_H, it is favorable to deposit charges outside the edge. This can be done without paying exchange energy by a relative shift of the Fermi momenta of spin-up and spin-down particles, as depicted in figure 2. In the absence of Zeeman splitting, $\varepsilon_Z = 0$, this is a second-order phase transition with spontaneous breaking of the spin symmetry. Then, the distance between the two Fermi momenta varies as $k_{F2} - k_{F3} \propto (|V_H'| - V_c')^{1/2}$, eventually saturating at $\sim 1/l_B$ [29]. For finite Zeeman

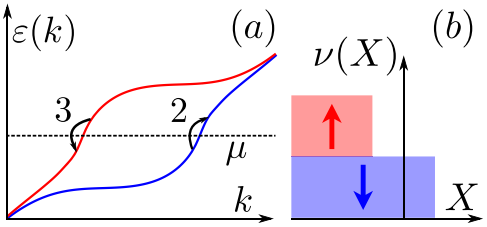

Figure 2. Spin reconstructed edge for $\varepsilon_Z = 0$. (a) Depicts the Hartree–Fock single-particle dispersion in the reconstructed region. Note that we set the curvature of the confinement potential to zero such that the velocity difference $v_2 - v_3 > 0$ is not obvious from the figure. (b) Shows the $T = 0$ occupation numbers of the different spin species in terms of the guiding center coordinate X.

splitting ε_Z, the spin symmetry is lifted by the Zeeman field and the transition is smeared on the scale of $k_{F2} - k_{F3} \sim \varepsilon_Z / v_2$.

Spin reconstruction leads to characteristic changes in the single-particle dispersion that develops an 'eye structure' (see figure 2(a)). Important for the relaxation dynamics is the increase of $v_2 - v_3 = (k_{F2} - k_{F3})/m_c$, which enhances the typical energy transferred per step of relaxation (see equation (4)).

For truly long-range interactions, the Hartree–Fock approximation predicts a logarithmic singularity $\sim e^2/\kappa \ln(|k - k_F| l_B)$ of the particle velocity at the Fermi energy, which is however cut off in the presence of screening, say by a nearby gate electrode. The Fermi velocity is thus still of the order of v_2, $v_3 \sim e^2/\kappa$ for typical choices of the screening length.

Even with spin reconstruction, the relaxation of hot particles can be described within the model dispersion of equation (3). We consider the case when the hot particle (not shown in figure 2) is injected well outside the energy window $e^2/(\kappa l_B)$ of the reconstructed region. This is compatible with the condition for validity of a perturbative expansion, which reduces to $v_1 \gg v_2$ for the case of the Fermi velocity determined by the interaction.

The energy relaxation rate $1/\tau_E^{(s)}$ can now be derived in the same way as for the unreconstructed edge, and consequently, equation (10) applies also to spin reconstructed edges. The crucial difference is that the velocity difference $v_2 - v_3$ is now strongly enhanced by the spin reconstruction, taking values up to $v_2 - v_3 \sim 1/(m_c l_B)$. Comparing the rates before $[v_2 - v_3 \sim \max\{\varepsilon_Z, T\}/(m_c v_2)]$ and well after spin reconstruction, we find an enhancement of the relaxation rates given by

$$\frac{1}{\tau_E^{(s)}} \sim \left(\frac{e^2/(\kappa l_B)}{\max\{\varepsilon_Z, T\}} \right)^2 \frac{1}{\tau_E^{(u)}}. \tag{13}$$

4. Charge reconstruction

For confinement potentials that vary even more smoothly, changing by $e^2/\kappa l_B$ over a region $w > l_B$, charge reconstruction may occur such that some of the electrons at the edge are pushed away from the bulk by a length of the order of l_B [31, 32]. It leads to nonmonotonic behavior

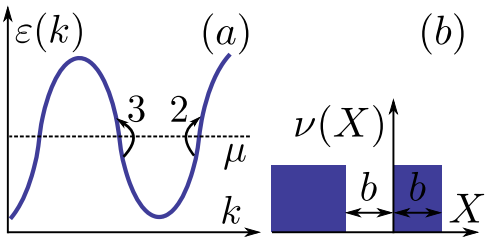

Figure 3. Charge reconstructed edge. (a) Depicts the Hartree–Fock single-particle dispersion in the reconstructed region of a spin polarized sample at $\nu = 1$. (b) Shows the occupation number near the edge of the sample.

of the dispersion with momentum and the creation of two additional counter-propagating[5] edge modes, as depicted in figure 3.

A minimal model for charge reconstruction considers filling factor $\nu = 1$ within the Hartree–Fock approximation [31]. It is convenient to formally model the confinement potential by a positive background charge which is distributed spatially as if it was occupying the lowest Landau-level wave functions ψ_X with occupation numbers $\nu_c(X) = \Theta(-X)$. The advantage of this model is that such a confinement potential exactly cancels the Hartree potential of the electrons for an unreconstructed edge. In this case, the electron occupation of the unreconstructed edge is stabilized by the (attractive) exchange potential.

The reconstruction transition can then be modeled by changing the abrupt drop of $\nu_c(X)$ into a linear decrease over a length w. For the unreconstructed electron occupations, this leads to negative (at $X < 0$) and positive (at $X > 0$) excess charges, causing a dipole field that favors separating electrons from the bulk. Once this dipole field overcomes the exchange potential, a charge reconstruction transition takes place. Within the Hartree–Fock approximation, this happens for $w \sim 8l_B$. Due to the particle–hole symmetric choice of the confinement potential around $X = 0$, the width and distance of the additional stripe from the bulk electron droplet both take the same value b. Moreover, the transition is of first order in the sense that b changes abruptly at the transition from zero to a value of the order of l_B.

Note that the same mechanism induces new (weaker) effective dipole fields at each of the three Fermi points as the edge becomes yet smoother. Thus, increasing w even further causes additional stripes to appear, eventually approaching the limit of a compressible edge which is expected for $w \gg l_B$ [23]. In the following we will focus on $w \gtrsim l_B$, remaining well outside the compressible limit.

Energy relaxation in the charge reconstructed case can also be captured by the dispersion (3) when setting $v_3 < 0$ and choosing the particle $i = 2$ to lie in one of the co-propagating branches[6]. The three Fermi velocities of the charge reconstructed edge are essentially determined by the variation of the exchange potential, which is short range such that $b \gtrsim l_B$ already approximates the bulk edge ($b \to \infty$) behavior. Consequently, the magnitudes of the

[5] Note that the conductance may stay at the $\nu = 1$ level due to impurity-induced elastic backscattering of electrons at the Fermi level. At higher energies, inelastic scattering leads to a shorter mean free path and we can therefore omit the disorder-induced backscattering.

[6] Processes where the particle $i = 2$ is on the inner or outer co-propagating branch contribute at the same order in the power counting argument. The choice depicted in figure 3 is slightly favored because of a larger Coulomb matrix element due to the shorter distance to the hot particle.

Fermi velocities are equal to that of the unreconstructed edge and $\sim e^2/\kappa$. In line with the discussions above, we consider the relaxation of a hot particle injected well outside the reconstructed region with $v_1 \gg e^2/\kappa$.

The nonmonotonic behavior of the dispersion introduces a new relaxation process which relaxes the hot particle by exciting two counter-propagating electron–hole pairs (see figure 3). This eliminates the restriction that the energy transfers at the Fermi energy cannot exceed the temperature, and makes the relaxation process similar to that for nonchiral quantum wires [26]. Unlike for quantum wires, however, the momentum transfers at the Fermi energy of the co- and counter-propagating branches are of the same order.

The three-body matrix element of equation (8) still applies in the presence of charge reconstruction because its derivation did not require a specific sign of v_3. Note, however, that for the charge reconstructed case $v_2 - v_3 \sim v_2 \sim e^2/\kappa$ and is therefore not connected to $k_{F2} - k_{F3} \sim 1/l_B$ by the curvature of the confinement potential. Assuming that there are no substantial curvature effects on the scale of the reconstructed region $V_c'' l_B^2 \ll e^2/(\kappa l_B)$ the last term of equation (8) dominates the three-body matrix element and equation (9) modifies to

$$T^{123}_{1'2'3'} = -\frac{2e^2}{L^2\kappa(\Delta k)^2}\frac{e^2/(\kappa l_B)}{(V_c'' l_B^2)^2 l_B^2} V_{q_1}(\Delta k). \tag{14}$$

The crucial difference for the energy relaxation rates compared to the unreconstructed case arises from the large allowed momentum $q_3 \sim 1/l_B$, which is limited only by the size of the reconstructed region for which the linearized dispersion applies. This increases both the momentum phase space to $(L/l_B)^3$ and the typical relaxed momentum to $(v_2 - v_3)/[(v_1 - v_2)l_B]$. Moreover, excitation and relaxation processes no longer need to be balanced when $e^2/\kappa l_B \gg T$, and we find

$$\frac{1}{\tau_E^{(c)}} \sim \left(\frac{e^2/(\kappa l_B)}{V_c'' l_B^2}\right)^3 \sqrt{\varepsilon V_c'' l_B^2} \left(\frac{e^2/(\kappa l_B)}{\varepsilon}\right)^4, \tag{15}$$

which applies for $\varepsilon \gg (e^2/\kappa l_B)^2/(V'' l_B^2)$ and allows for relaxation even at $T = 0$. Equation (15) implies that the increased phase space and the energy relaxation step size lead to a dramatic enhancement of the relaxation rate compared to the unreconstructed case (see equation (12)) as

$$\frac{1}{\tau_E^{(c)}} \sim \sqrt{\frac{\varepsilon}{V'' l_B^2}} \left(\frac{e^2/(\kappa l_B)}{V_c'' l_B^2}\right)^3 \left(\frac{e^2/(\kappa l_B)}{T}\right)^6 \frac{1}{\tau_E^{(u)}}, \tag{16}$$

where we used the limit $T \gg \varepsilon_Z$.

To obtain an estimate of the relaxation rates, we assume that $V_c'' l_B^2$ is of the order of the Coulomb interaction scale $e^2/(\kappa l_B)$, say, $e^2/(\kappa l_B) \sim 30\,\mathrm{K}$ for $B = 5\,\mathrm{T}$. Then, we find relaxation lengths of the order of micrometers for excitation energies of the order of $\omega_c \sim 100\,\mathrm{K}$. The experiments in [7–9] are conducted at significantly lower excitation energies $< 1\,\mathrm{K}$, making real collisions conserving both energy and momentum an unlikely origin of the observed relaxation.

5. Conclusions

We studied three-body processes as an intrinsic mechanism for relaxation of hot electrons in clean integer quantum Hall edges at Landau-level filling factors $\nu = 1$ and 2. These processes rely crucially on the form of the electron dispersion and are thus susceptible to edge reconstruction effects. For an unreconstructed edge, energy relaxation requires a finite

temperature which determines the phase space for the relaxation processes. The energy given up by the hot electron in a single three-body collision is controlled by curvature effects on the scale of temperature or Zeeman energy so that the relaxation rate can be tuned by a magnetic field once $\varepsilon_Z \gg T$.

While unreconstructed edges are expected for steep confinement potentials, smoother confinement potentials with $V_c' \lesssim e^2/(\kappa l_B^2)$ may lead to an interaction-induced spin reconstruction, which causes a relative shift of the Fermi momenta of the two spin species by $\sim 1/l_B$. The three-body processes are then controlled by curvature effects on the scale of the interaction energy $e^2/(\kappa l_B)$, which causes a strong increase of the relaxation rate (see equation (13)).

Even softer confinement may cause charge reconstruction, which introduces additional co- and counter-propagating edge modes. The presence of counter-propagating modes allows for relaxation even at $T = 0$. Consequently, the phase space for three-body collisions is no longer controlled by temperature but by the size of the reconstructed region $\sim e^2/(\kappa l_B)$, which ensures an additional dramatic enhancement of the relaxation rate (see equation (16)).

Experimental studies of interaction-induced reconstruction transitions in high magnetic fields have been performed [24]. Our study suggests that it would be rewarding to experimentally investigate relaxation processes in such systems.

Acknowledgments

We acknowledge financial support from the Deutsche Forschungsgemeinschaft under SPP 1538 (FUB) and by DOE under contract no. DEFG02-08ER46482 (Yale) and by the US–Israel BSF under grant no. 2010366 (Yale). AL acknowledges support from Michigan State University.

Appendix A. Calculation of the Coulomb matrix element $V_q(k_1 - k_2)$

Within this section we provide all essential details needed for the derivation of equation (7) presented in the main text. We assume that the edge is smooth enough that we can approximate the electron wave functions by those of the bulk. We start from the interaction matrix element in real space

$$V_{\mathrm{d}X}(X, X') = \left\langle \psi^{(1)}_{X+\mathrm{d}X}, \psi^{(2)}_{X'-\mathrm{d}X} \left| \frac{e^2/\kappa}{|\mathbf{r}^{(1)} - \mathbf{r}^{(2)}|} \right| \psi^{(1)}_{X}, \psi^{(2)}_{X'} \right\rangle. \tag{A.1}$$

In the following, we will measure all length scales in units of magnetic length l_B. In these units the guiding center coordinate directly translates to momenta. With the lowest Landau-level wave functions of equation (1), we then find that

$$V_{\mathrm{d}X}(X, X') = \frac{e^2}{\pi\kappa L^2} \int \mathrm{d}x\, \mathrm{d}y\, \mathrm{d}\Delta x\, \mathrm{d}\Delta y \frac{\mathrm{e}^{-\sqrt{\Delta x^2+\Delta y^2}/\lambda}}{\sqrt{\Delta x^2+\Delta y^2}} \mathrm{e}^{-\mathrm{i}\Delta y\, \mathrm{d}X} \mathrm{e}^{-\frac{1}{2}(x-X)^2} \mathrm{e}^{-\frac{1}{2}(x-X-\mathrm{d}X)^2} \times \mathrm{e}^{-\frac{1}{2}(x+\Delta x-X')^2} \mathrm{e}^{-\frac{1}{2}(x+\Delta x-X'+\mathrm{d}X)^2}, \tag{A.2}$$

where we used the screened Coulomb potential which carries an extra factor $\mathrm{e}^{-\sqrt{\Delta x^2+\Delta y^2}/\lambda}$ with λ being the distance to a screening gate. The integration over Δy gives $2K_0(|\Delta x\, \mathrm{d}X|)$ in the case when $\mathrm{d}X \gg 1/\lambda$, where K_0 is the Bessel function of imaginary argument. If, however, $\mathrm{d}X \ll 1/\lambda$ the integral is cut off and the result changes to $2K_0(|\Delta x/\lambda|)$. We will derive

results for the $\mathrm{d}X \gg 1/\lambda$ case and keep in mind appropriate changes for the other limit. After y integration, which gives a factor of L, we obtain the intermediate step

$$V_{\mathrm{d}X}(X, X') = \frac{2e^2}{\pi\kappa L}\mathrm{e}^{-\frac{1}{2}\mathrm{d}X^2}\int \mathrm{d}x\,\mathrm{d}\Delta x\, K_0(|\Delta x\,\mathrm{d}X|)\mathrm{e}^{-\frac{1}{2}(2x-X-X'+\Delta x)^2}\mathrm{e}^{-\frac{1}{2}(X-X'+\mathrm{d}X+\Delta x)^2}. \tag{A.3}$$

Performing now the Gaussian integral over x, which gives a factor of $\sqrt{\pi/2}$, followed by using the Landau gauge to replace guiding center coordinates by momenta, one arrives at

$$V_q(k) = \sqrt{\frac{2}{\pi}}\frac{e^2}{\kappa}\mathrm{e}^{-q^2/2}\int \mathrm{d}\xi\ \mathrm{e}^{-\frac{1}{2}(k+q+\xi)^2}K_0(|\xi q|), \tag{A.4}$$

where we used the short-hand notation $X - X' = kl_B^2 = k$ (with $l_B = 1$). Note that $V_q(k) = V_q(-k-2q)$ and is therefore not symmetric, which plays an important role. We see immediately that scattering processes with large momentum transfer $q \gg 1$ are exponentially suppressed. We therefore concentrate on the opposite limit of $q \ll 1$ when the exponential prefactor $\mathrm{e}^{-q^2/2}$ can be set to unity.

Let us study limiting cases of equation (A.4). In the case when $k \gg 1$, one can approximate the exponential under the integral by the delta-function $\sqrt{2\pi}\delta(k+q+\xi)$ and thus obtain

$$V_q(k) = \frac{2e^2}{\kappa}K_0(|q(k+q)|). \tag{A.5}$$

Using the asymptotic form of the Bessel function and restoring units of l_B, one recovers the second limit in equation (7).

In the other limiting case when $k \ll 1$, one can approximate the exponential under the integral of equation (A.4) by $\mathrm{e}^{-\xi^2/2}$ and then complete integration exactly with the result

$$V_q(k) = \frac{e^2}{\kappa}K_0(q^2/4). \tag{A.6}$$

With the logarithmic accuracy at small q this translates into the first limit of equation (7).

Appendix B. Calculation of the three-body matrix element $T^{123}_{1'2'3'}$

In general, the three-particle scattering amplitude $\langle 1'2'3'|VG_0V|123\rangle_c$ contains six terms: one direct and five exchange contributions [28]. As explained in the text, we need only the former one, which reads explicitly [28]

$$\begin{aligned} T^{123}_{1'2'3'} = \frac{\delta_{\Sigma,\Sigma'}}{L^2}\Bigg[&\frac{V_{k_{3'}-k_3}(k_3-k_2)V_{k_{1'}-k_1}(k_{2'}-k_{1'})}{\varepsilon_{k_3}+\varepsilon_{k_2}-\varepsilon_{k_{3'}}-\varepsilon_{k_2+k_3-k_{3'}}} + \frac{V_{k_{1'}-k_1}(k_1-k_3)V_{k_{2'}-k_2}(k_{3'}-k_{2'})}{\varepsilon_{k_1}+\varepsilon_{k_3}-\varepsilon_{k_{1'}}-\varepsilon_{k_3+k_1-k_{1'}}} \\ &+ \frac{V_{k_{2'}-k_2}(k_2-k_1)V_{k_{3'}-k_3}(k_{1'}-k_{3'})}{\varepsilon_{k_2}+\varepsilon_{k_1}-\varepsilon_{k_{2'}}-\varepsilon_{k_1+k_2-k_{2'}}} + \frac{V_{k_{2'}-k_2}(k_2-k_3)V_{k_{1'}-k_1}(k_{3'}-k_{1'})}{\varepsilon_{k_2}+\varepsilon_{k_3}-\varepsilon_{k_{2'}}-\varepsilon_{k_3+k_2-k_{2'}}} \\ &+ \frac{V_{k_{1'}-k_1}(k_1-k_2)V_{k_{3'}-k_3}(k_{2'}-k_{3'})}{\varepsilon_{k_1}+\varepsilon_{k_2}-\varepsilon_{k_{1'}}-\varepsilon_{k_2+k_1-k_{1'}}} + \frac{V_{k_{3'}-k_3}(k_3-k_1)V_{k_{2'}-k_2}(k_{1'}-k_{2'})}{\varepsilon_{k_3}+\varepsilon_{k_1}-\varepsilon_{k_{3'}}-\varepsilon_{k_1+k_3-k_{3'}}}\Bigg], \end{aligned} \tag{B.1}$$

where the spin structure is $\delta_{\Sigma,\Sigma'} = \delta_{\sigma_1,\sigma_{1'}}\delta_{\sigma_2,\sigma_{2'}}\delta_{\sigma_3,\sigma_{3'}}$ and the Coulomb matrix element $V_q(k)$ was derived in appendix A. Now using the dispersion relation from equation (3) and the constraint

on momentum transfers from equation (4) imposed by the conservation laws, one can simplify $T^{123}_{1'2'3'}$ to

$$T^{123}_{1'2'3'} \approx \frac{\delta_{\Sigma,\Sigma'}}{L^2}\left[\frac{V_{q_3}(k_3-k_2)V_{q_1}(k_1-k_2+q_3)-V_{q_1}(k_1-k_2)V_{q_3}(k_3-k_2+q_1)}{q_3(v_2-v_3)}\right.$$
$$+\frac{V_{q_2}(k_2-k_3)V_{q_1}(k_1-k_3+q_2)-V_{q_1}(k_1-k_3)V_{q_2}(k_2-k_3+q_1)}{q_2(v_3-v_2)}$$
$$\left.+\frac{V_{q_3}(k_3-k_1)V_{q_2}(k_2-k_1+q_3)-V_{q_2}(k_2-k_1)V_{q_3}(k_3-k_1+q_2)}{q_3(v_1-v_3)}\right], \tag{B.2}$$

where we used the property $V_q(k) = V_q(-k-2q)$. It is important to stress that the above expression would vanish by ignoring the dependence of the Coulomb matrix element on initial momenta, namely for $V_q(k) = V_q$. To proceed further we make use of the assumption that the injected particle is of high energy, such that $v_1 \gg v_{2,3}$ and $k_1 \gg k_{2,3}$. In this case we expand $V_{q_i}(\Delta k + q_i)$ in q_i. For the interaction $V_q(k) = -\frac{2e^2}{\kappa}\ln(|kq|l_B^2)$, we obtain after the expansion

$$T^{123}_{1'2'3'} \approx \frac{2e^2\delta_{\Sigma,\Sigma'}}{\kappa L^2}\left[-\frac{V_{q_3}(k_3-k_2)}{(v_2-v_3)(k_1-k_2)}-\frac{V_{q_1}(k_1-k_2)}{(v_1-v_2)(k_2-k_3)}+\frac{V_{q_2}(k_2-k_3)}{(v_2-v_3)(k_1-k_3)}\right.$$
$$\left.+\frac{V_{q_1}(k_1-k_3)}{(v_1-v_3)(k_2-k_3)}+\frac{V_{q_3}(k_3-k_1)}{(v_1-v_3)(k_1-k_2)}+\frac{V_{q_2}(k_2-k_1)}{(v_1-v_2)(k_1-k_3)}\right]. \tag{B.3}$$

Note that if we are in the regime when $k_2 - k_3 \ll l_B^{-1}$ we have to use the interaction potential $V_q(k) = -\frac{2e^2}{\kappa}\ln(|q|l_B)$, which has a vanishing derivative with respect to k. This can be accounted for by removing the two terms with $V_{q_1}(\ldots)$ in the above formula for $T^{123}_{1'2'3'}$. Finally, to leading logarithmic order we can set $V_{q_1}(k_1-k_2) = V_{q_1}(k_1-k_3)$ as well as $V_{q_2}(k_2-k_1) = V_{q_3}(k_3-k_1) = V_{q_3}(k_1-k_2)$ and $V_{q_3}(k_3-k_2) = V_{q_2}(k_2-k_3)$ to obtain equation (8) since the spin summation is equal to unity.

References

[1] Deshpande V V, Bockrath M, Glazman L I and Yacoby A 2010 *Nature* **464** 209
[2] Imambekov A, Schmidt T L and Glazman L I 2011 arXiv:1110.1374
Imambekov A, Schmidt T L and Glazman L I 2011 *Rev. Mod. Phys.* submitted
[3] Barak G, Steinberg H, Pfeiffer L N, West K W, Glazman L, von Oppen F and Yacoby A 2010 *Nature Phys.* **6** 489
[4] Chen Y-F, Dirks T, Al-Zoubi G, Birge N O and Mason N 2009 *Phys. Rev. Lett.* **102** 036804
[5] Kinoshita T, Wenger T and Weiss D S 2006 *Nature* **440** 900
[6] Hofferberth S, Lesanovsky I, Fischer B, Schumm T and Schmiedmayer J 2007 *Nature* **449** 324
[7] Altimiras C, le Sueur H, Gennser U, Cavanna A, Mailly D and Pierre F 2010 *Nature Phys.* **6** 34
[8] le Sueur H, Altimiras C, Gennser U, Cavanna A, Mailly D and Pierre F 2010 *Phys. Rev. Lett.* **105** 056803
[9] Altimiras C, le Sueur H, Gennser U, Cavanna A, Mailly D and Pierre F 2010 *Phys. Rev. Lett.* **105** 226804
[10] Paradiso N, Heun S, Roddaro S, Sorba L, Beltram F and Biasiol G 2011 *Phys. Rev.* B **84** 235318
[11] Granger G, Eisenstein J P and Reno J L 2009 *Phys. Rev. Lett.* **102** 086803
[12] Wen X G 1990 *Phys. Rev. Lett.* **64** 2206
Wen X G 1991 *Phys. Rev.* B **43** 11025
[13] Kane C L and Fisher M P A 1994 *Phys. Rev.* B **51** 13449
Kane C L and Fisher M P A 1995 *Phys. Rev.* B **52** 17393
Kane C L and Fisher M P A 1997 *Phys. Rev.* B **55** 15832

[14] Lunde A M, Nigg S E and Büttiker M 2010 *Phys. Rev.* B **81** 041311
[15] Degiovanni P, Grenier C, Fève G, Altimiras C, le Sueur H and Pierre F 2010 *Phys. Rev.* B **81** 121302
[16] Kovrizhin D L and Chalker J T 2011 *Phys. Rev.* B **84** 085105
[17] Kovrizhin D L and Chalker J T 2011 arXiv:1111.3914
[18] Levkivskyi I P and Sukhorukov E V 2012 *Phys. Rev.* B **85** 075309
[19] Ji Y, Chung Y, Sprinzak D, Heiblum M, Mahalu D and Shtrikman H 2003 *Nature* **422** 415
[20] Neder I, Heiblum M, Levinson Y, Mahalu D and Umansky V 2006 *Phys. Rev. Lett.* **96** 016804
[21] Heyl M, Kehrein S, Marquardt F and Neuenhahn C 2010 *Phys. Rev.* B **82** 033409
[22] Halperin B I 1982 *Phys. Rev.* B **25** 2185
[23] Chklovskii D B, Shklovskii B I and Glazman L I 1992 *Phys. Rev.* B **46** 4026
[24] Barak G, Pfeiffer L N, West K W, Halperin B I and Yacoby A 2010 arXiv:1012.1845
[25] Deviatov E V, Lorke A, Biasiol G and Sorba L 2011 *Phys. Rev. Lett.* **106** 256802
[26] Karzig T, Glazman L I and von Oppen F 2010 *Phys. Rev. Lett.* **105** 226407
[27] Micklitz T and Levchenko A 2011 *Phys. Rev. Lett.* **106** 196402
[28] Lunde A, Flensberg K and Glazman L I 2007 *Phys. Rev.* B **75** 245418
[29] Dempsey J, Gelfand B Y and Halperin B I 1993 *Phys. Rev. Lett.* **70** 3639
[30] Stoof T H and Bauer G E W 1995 *Phys. Rev.* B **52** 12143
[31] Chamon C de C and Wen X G 1994 *Phys. Rev.* B **49** 8227
[32] Barlas Y, Joglekar Y N and Yang K 2011 *Phys. Rev.* B **83** 205307